Published in final edited form as:
Sci Transl Med. 2013 November 27; 5(213): 213ra167. doi:10.1126/scitranslmed.3007049.

Transepithelial Transport of Fc -Targeted Nanoparticles by the Neonatal Fc Receptor for Oral Delivery

Eric M. Pridgen[1,2,†], **Frank Alexis**[3,4,†], **Timothy T. Kuo**[5], **Etgar Levy-Nissenbaum**[3,4], **Rohit Karnik**[6], **Richard S. Blumberg**[5], **Robert Langer**[1,2,4], and **Omid C. Farokhzad**[3,4,*]

[1]Department of Chemical Engineering, Massachusetts Institute of Technology, Cambridge, MA 02139

[2]The David H. Koch Institute for Integrative Cancer Research, Cambridge, MA 02139

[3]Laboratory of Nanomedicine and Biomaterials, Department of Anesthesiology, Brigham and Women's Hospital, Harvard Medical School, Boston, MA 02115

[4]MIT-Harvard Center for Cancer Nanotechnology Excellence, Cambridge, MA 02139

[5]Division of Gastroenterology, Department of Medicine, Brigham and Women's Hospital, Harvard Medical School, Boston, MA 02115

[6]Department of Mechanical Engineering, Massachusetts Institute of Technology, Cambridge, MA 02139

Abstract

Nanoparticles are poised to have a tremendous impact on the treatment of many diseases, but their broad application is limited because currently they can only be administered by parenteral methods. Oral administration of nanoparticles is preferred but remains a challenge because transport across the intestinal epithelium is limited. Here, we show that nanoparticles targeted to the neonatal Fc receptor (FcRn), which is known to mediate the transport of IgG antibodies across epithelial barriers, are efficiently transported across the intestinal epithelium using both *in vitro* and *in vivo* models. In mice, orally administered FcRn-targeted nanoparticles crossed the intestinal epithelium and reached systemic circulation with a mean absorption efficiency of 13.7%*h compared with only 1.2%*h for non-targeted nanoparticles. In addition, targeted nanoparticles containing insulin as a model nanoparticle-based therapy for diabetes were orally administered at a clinically relevant insulin dose of 1.1 U/kg and elicited a prolonged hypoglycemic response in wild-type mice. This effect was abolished in FcRn knockout mice, indicating the enhanced nanoparticle transport was due specifically to FcRn. FcRn-targeted nanoparticles may have a

*To whom correspondence should be addressed: ofarokhzad@zeus.bwh.harvard.edu.
†These authors contributed equally to this work

Author Contributions: E.M.P and F.A. designed and performed the experiments, analyzed the data, did the statistical analysis, and wrote the manuscript; O.C.F. designed the experiments, analyzed the data, and wrote the manuscript; R.L., R.K., and R.S.B. designed the experiments, analyzed the data, and critically reviewed the manuscript; T.T.K and E.L-N. analyzed the data and critically reviewed the manuscript.

Competing interests: O.C.F. and R.L. have financial interests in BIND Therapeutics, Selecta Biosciences, and Blend Therapeutics, which are developing nanoparticle therapeutics.

major impact on the treatment of many diseases by enabling drugs currently limited by low bioavailability to be efficiently delivered though oral administration.

Introduction

Nanoparticles (NPs) have the potential to make a significant impact on the treatment of many diseases, including cancer, cardiovascular disease, and diabetes. Many NP-based therapeutics are now entering clinical trials or have been approved for use (1, 2), including targeted polymeric nanoparticles ((3), clinical trial NCT01478893) based on technologies that we have previously described (4). However, the impact of NPs in the clinic may be limited to a narrow set of indications because NP administration is currently restricted to parenteral methods. Many diseases that could benefit from NP-based therapeutics require frequent administration. Alternate routes of administration, particularly oral, are preferred because of the convenience and compliance by patients (5). Intestinal absorption of NPs is highly inefficient because the physicochemical parameters of NPs prevent their transport across cellular barriers such as the intestinal epithelium (6). To improve the absorption efficiency of NPs and to make the oral administration of NPs practical in the clinic, new strategies are necessary to overcome the intestinal epithelial barrier.

The neonatal Fc receptor (FcRn) mediates IgG transport across polarized epithelial barriers (7, 8). It was discovered as the receptor in the neonatal intestine that transports IgG in breast milk from mother to offspring (9). However, FcRn is expressed into adulthood at levels similar to fetal expression in the apical region of epithelial cells in the small intestine and diffusely throughout the colon (10). FcRn is also expressed in the vascular endothelium, blood-brain barrier, kidneys, liver, lungs, and throughout the hematopoietic system (11, 12). FcRn interacts with the Fc portion of IgG in a pH-dependent manner, binding with high affinity in acidic (pH <6.5) but not physiological environments (pH ~7.4) (13). The intracellular trafficking of the IgG:FcRn complex has been conclusively demonstrated in the rat intestine using IgG Fc labeled with 1.4-nm gold as a contrast agent for electron tomography (14). The studies revealed that Fc is transported through a complex pathway involving a network of entangled tubular and irregular vesicles in order to reach the basolateral surface of the cell.

We hypothesized that targeting NPs to FcRn using IgG Fc fragments would allow orally administered NPs to be transported across the intestinal epithelium in rodents (Fig. 1). In acidic sections of the intestine, such as the duodenum and portions of the jejunum (15), Fc fragments conjugated to NPs [Fc-targeted NPs (NP-Fc)] will bind to FcRn at the apical surface of absorptive epithelial cells, leading to receptor-mediated endocytosis (16). NP-Fc could also be taken up by fluid phase pinocytosis. During intracellular trafficking, NP-Fc and FcRn in the same acidic endosome compartments will bind with high affinity. FcRn can then guide bound NP-Fc through a transcytosis pathway, avoiding lysosomal degradation (17). On the basolateral side, exocytosis results in exposure to a neutral pH environment in the lamina propria, causing the release of NP-Fc (18). NP-Fc can then diffuse through the lamina propria and enter systemic circulation.

Fc-fusion proteins have been used to overcome biological barriers: Fc fused with erythropoietin was measured in non-human primates (19) and humans (20) after pulmonary administration, indicating that using the FcRn is a valid transport pathway in humans; and follicle-stimulating hormone fused with Fc reached circulation after oral delivery in newborn rats (21). However, NPs offer several potential advantages over fusion proteins including (i) transport of many drug molecules with each transcytosis event; (ii) protection of drug molecules, particularly protein therapeutics, through encapsulation; and (iii) mitigation of the need for drug modification. Recently, 20–50-nm fluorescent NPs conjugated to IgG Fc were transported across an *in vitro* airway epithelial cell monolayer (22). Yet no studies, to our knowledge, have used drug-encapsulated NPs to target the FcRnfor oral drug delivery applications.

Herein, we developed polymeric NPs surface-modified with Fc to target FcRn, resulting in transepithelial transport both *in vitro* and *in vivo*. NP-Fc demonstrated enhanced transport specifically mediated by FcRn across an intestinal epithelial monolayer *in vitro*. In mice, NP-Fc were imaged crossing the intestinal epithelium and entering the lamina propria after oral administration. NP-Fc were also measured in several organs after oral administration, indicating that NP-Fc were able to reach systemic circulation. Finally, NP-Fc encapsulating insulin as a model NP-based therapeutic for diabetes were administered orally and elicited a hypoglycemic response. These results demonstrate that NPs targeted to the FcRn are capable of crossing an epithelial barrier *in vivo* using a transcytosis pathway.

Results

Preparation of Fc-Targeted Nanoparticles

NPs were formed from biodegradable and biocompatible poly(lactic acid)–*b*-poly(ethylene glycol) (PLA-PEG) block copolymers. PLA is a biodegradable polymer used in many FDA-approved products and forms the NP core owing to its hydrophobicity. PEG is a biocompatible polymer that remains on the NP surface owing to its hydrophilic nature and forms the NP corona. PLA-PEG was synthesized using ring-opening polymerization with a free terminal maleimide group (PLA-PEG-MAL) to conjugate the Fc portion of IgG.

Studies of NPs have shown enhanced intestinal uptake as particle size decreases (23, 24). However, these previous studies on particle size have mostly focused on nonspecific uptake by M cells in the Peyer's patches as opposed to specifically targeting the NPs to a transcytosis pathway such as the FcRn-mediated pathway. Here, the nanoprecipitation self-assembly method (25)(Fig. 2A) was used to generate particles with a mean hydrodynamic diameter of 55 nm and a polydispersity of 0.05 (Fig. 2B).

Polyclonal IgG Fc fragments were covalently conjugated to PEG using maleimide-thiol chemistry. 2-Iminothiolane was used to modify the Fc with thiol groups (Fc-SH). Fc-SH was incubated with NPs for conjugation (Fig. 2A). The amount of Fc conjugated to the NPs was measured for both Fc-SH and unmodified Fc (Fig. 2C). Unmodified Fc resulted in a lower ligand density than Fc-SH, indicating minimal nonspecific interactions between Fc and the NP surface and that the unbound Fc was successfully separated from NP using centrifugal filtration. The ligand density for Fc-SH was 32-fold higher than unmodified Fc, indicating

that Fc was bound on the NP surface. In addition, the hydrodynamic diameter of the NP increased from 55 to 63 nm after Fc conjugation (Fig. 2B) - an increase consistent with the hydrodynamic diameter of IgG Fc (~3 nm) (26). The surface charge showed only a minor change from −4.3 ± 0.4 for NP to −5.6 ± 1.1 mV for NP-Fc (mean ± SD, n=3, $p>0.05$, Student's t test).

In vitro Transepithelial Transport

In vitro NP transepithelial transport studies were conducted using an epithelial cell monolayer model with Caco-2 cells, a human epithelial colorectal adenocarcinoma cell line typically used as a model of the intestine for drug permeability testing. Caco-2 cells endogenously express human FcRn and human beta-2-microglobulin, and have previously been used for IgG transcytosis studies (8, 27). ^{3}H-labeled NPs were used to measure transport across the Caco-2 monolayer. Using this system with a pH gradient established from the apical to basolateral side of the Caco-2 polarized monolayer (to mimic the physiological pH of the duodenum and enhance apical binding), the transcytosis of non-targeted NPs (control) and NP-Fc was measured. ^{3}H measurements for NP-Fc on the basolateral side were twofold greater than non-targeted NPs after 24 h, indicating that Fc on the NP surface significantly enhanced transepithelial transport *in vitro* (Fig. 2D). When NP-Fc was combined with a 50-fold excess of free IgG Fc as a blocking agent for the FcRn transcytosis pathway, NP-Fc transport was significantly reduced, indicating that the enhanced transport of NP-Fc is at least partially receptor-mediated (Fig. 2D).

FcRn Expression in Mice

FcRn expression throughout the entire small and large intestine of wild-type mice was confirmed by Western blot (Fig. 3A). Quantification of band intensity showed that the FcRn expression decreased in the distal sections of the small intestine and the colon (Fig 3B). Immunohistochemistry showed that FcRn was localized to the epithelium of the intestinal villi of the duodenum of wild -type mice (Fig 3C).

In vivo Absorption and Biodistribution

In vivo transport of NP-Fc across the intestinal epithelium was visualized using fluorescently labeled NPs. Fasted wild-type mice were orally administered the fluorescently labeled NPs, and sections of the duodenum were collected and analyzed using confocal fluorescence microscopy. Figure 3D shows representative images for both non-targeted NPs and NP-Fc. For the non-targeted NPs, the fluorescence from the NPs was not observed in the villi, suggesting that the NPs were unable to enter the villi. However, for the NP-Fc, fluorescence was observed inside the villi on the basolateral side of the epithelial cells, indicating that NP-Fc crossed the intestinal epithelium and entered the lamina propria(Fig. 3 D).

The biodistribution and absorption efficiency of both targeted and non-targeted NPs were quantitatively measured by radiolabeling the NPs with ^{14}C. Figure 4A shows the biodistribution of non-targeted NPs and NP-Fc over the course of 8 hours after oral administration to fasted wild-type mice. For the non-targeted NPs, a small amount of ^{14}C was measured in the organs. By contrast, a large amount of ^{14}C was measured in the spleen, kidneys, liver, and lungs for NP-Fc, indicating that NP-Fc entered systemic circulation after

oral administration and reached several organs known to express FcRn (11). The ^{14}C in the organs was transient, peaking at 2.5 h post-delivery and clearing from the organs at later time points (Fig. 4A). To ensure that the ^{14}C remained with the NPs over the course of the experiment, the release of ^{14}C from the NPs was measured and no release was observed over 24 h (Fig. 4B).

The total ^{14}C absorbed over time was calculated by summing the ^{14}C measured in each of the organs (spleen, kidneys, liver, heart, and lungs) at a specific time point (Fig. 4C). Significantly higher amounts of ^{14}C were absorbed for NP-Fc at 1.5, 2.5, and 4 h compared with non-targeted NPs, indicating that Fc targeting enhanced absorption. The area under the curve (AUC) was used to calculate the oral absorption efficiency, which was 1.2%*h ± 0.2 for non-targeted NPs and 13.7%*h ± 1.3 for NP-Fc (mean ± SEM with n=5 mice per timepoint; $P < 0.001$, Student's t test). This difference in AUC suggests that IgG Fc targeting was responsible for an 11.5-fold increase in NP absorption.

Oral Delivery of Insulin to Wild-type Mice

NP-Fc that are capable of encapsulating insulin were developed as a model NP-based therapeutic for diabetes that could be orally administered and evaluated for eliciting a pharmacologic response. Insulin NPs (insNP) were prepared using nanoprecipitation after dissolving insulin and PLA-PEG-MAL in dimethyl sulfoxide (DMSO), resulting in an insulin load of 0.5% (w/w). The nanoprecipitation method allowed the particle size to remain small (mean hydrodynamic diameter, 57 nm) while still allowing insulin encapsulation. The release of insulin from insNP in PBS at 37°C demonstrated a strong burst release in the first hour followed by a controlled release (Fig. 5A). The insulin release profile was advantageous because it allowed all of the insulin to be delivered before complete clearance of the particles after 10 h. To determine the bioactivity, insulin released from insNP was collected and injected into fasted wild-type mice by tail-vein injection. The bioactivity was measured by monitoring the blood glucose and comparing the response to an equivalent dose of free insulin solution (3.3 U/kg). The released insulin generated a hypoglycemic response in mice (Fig. 5B), indicating that the encapsulated insulin was bioactive after release from the insNP.

The hypoglycemic response generated after oral administration of the targeted insNP (insNP-Fc) was tested using fasted wild-type mice and compared with the efficacies of non-targeted insNP, free insulin, and NP-Fc without insulin (Fig. 5C). The free insulin administered orally did not generate a glucose response in the mice, unlike the free insulin injected into the tail vein that was able to generate a glucose response (Fig. 4B). The NP-Fc without insulin also was unable to generate a glucose response. The glucose response generated by non-targeted insNP was not different from that generated by the control groups at any time point. However, insNP-Fc caused a significant hypoglycemic response in the mice, reducing the glucose during the first 10 h after administration. This is consistent with the biodistribution (Fig. 4A) and insulin release data (Fig. 5A), which demonstrated that the particles were cleared and the insulin was released within 10 h, respectively. The blood glucose level then increased and was similar to that of the control groups by 15 h. The insNP-Fc insulin dose required to generate the hypoglycemic response was 1.1 U/kg, which

is clinically relevant (28) and lower than other oral insulin delivery systems that require 10–100 U/kg to generate a glucose response (29). When compared with the glucose response from free insulin administered by tail vein injection (Fig. 5B), the orally administered insNP-Fc resulted in a prolonged (15 h vs. 1.5 h) hypoglycemic response (Fig. 5C).

To demonstrate that the enhanced hypoglycemic response generated by insNP-Fc was due specifically to the IgG Fc ligand on the NP surface, several additional control groups were tested. The first control was to administer insNP-Fc concurrently with a 50-fold excess of free IgG Fc. The second control was to conjugate chicken IgY Fc fragments to insNP instead of human IgG Fc fragments. [Chicken IgY is the functional equivalent of IgG in non-mammalian species such as birds, but does not bind to mouse FcRn (30).] Both control groups had hypoglycemic responses that were significantly less than insNP-Fc (Fig. 5D), indicating that the use of the IgG Fc as a targeting ligand was responsible for the enhanced hypoglycemic response.

Oral Delivery of Insulin to FcRn Knockout Mice

The role of FcRn in NP transepithelial transport was tested by repeating the efficacy experiment using FcRn knockout (KO) mice. FcRn KO mice had the same insulin sensitivity as the wild-type mice, so the same insulin dose was used for both strains (Fig. 5E). In contrast to the results in the wild-type mice (Fig. 5C), insNP-Fc did not generate a hypoglycemic response significantly different from the other three groups in the FcRn KO mice (Fig. 5F). In these FcRn KO mice, the response generated by insNP-Fc resembled the response generated by non-targeted insNP in the wild-type mice (Fig. 5C), suggesting that the benefit gained from using Fc was specifically due to FcRn.

In vivo Glucose Response Dose-Dependency

The glucose response in both wild-type and FcRn KO mice was evaluated for dose dependency using two different doses of insNP-Fc: 0.66 U/kg and 1.1 U/kg (Fig. 5G). For the FcRn KO mice, there was no difference in the glucose response between the two doses of insNP-Fc. However, for the wild-type mice, the glucose response was significantly greater at the higher dose of insNP-Fc, suggesting a possible dose-dependence in the wild-type mice.

Discussion

For many diseases, oral administration of therapeutics is the standard of care because daily therapy is required. In some cases, chronic diseases, such as cancer, that have been treated in the clinic with intravenous infusions are now increasingly being treated with oral therapeutics because patients prefer the convenience of oral administration relative to parenteral administration. For NP-based therapeutics to be a practical treatment of many diseases, NP formulations appropriate for oral administration are necessary. The most significant barrier to the effective oral administration of NPs is the intestinal epithelium, which limits the absorption of NPs. To date, there is no practical solution to this problem.

There have been many attempts to develop oral drug delivery systems that overcome this barrier (29). For example, permeation enhancers have been used to open tight junctions to

allow both paracellular and transcellular transport of drugs across the epithelium (31). Mucoadhesive biomaterials have been used to increase the retention time and local concentration of drugs near the apical surface of epithelial cells (32). Many oral NPs have been engineered for uptake by M cells in the Peyer's Patches, although this limits the surface area available for absorption and exposes NPs to underlying immune cells (33). Finally, a few NP formulations have targeted cell receptors, but they still suffer from low bioavailability and require high oral drug dosages (29, 34).

We have taken a novel approach to address this problem by developing drug encapsulated NPs capable of targeting FcRn for transepithelial transport and enhanced NP intestinal absorption after oral administration. FcRn has been shown to mediate the transcytosis of IgG across several epithelial and endothelial barriers (11), and more recently the transcytosis of fluorescent NPs was demonstrated across a monolayer of Calu-3 airway epithelial cells *in vitro* after adsorption of Fc on the NP surface (22). Harnessing the transcytosis pathway to cross the intestinal epithelium offers the advantage of leaving intact the integrity of the epithelial barrier, avoiding potential safety issues and adverse effects associated with manipulating the permeability of the intestine for paracellular or transcellular transport. An additional advantage of targeting the FcRn is that this receptor is expressed throughout the intestine, providing a significant increase in the available absorption surface area for NP-Fc, which is in contrast with other drug delivery systems that target only a specific portion of the intestine such as the Peyer's patches (6).

We have demonstrated that targeting FcRn for transepithelial transport by modifying the NP surface with IgG Fc provides a successful approach for the oral delivery of NPs. Using a mouse model, we demonstrated that FcRn enabled the NP-Fc to cross the intestinal epithelium and reach systemic circulation. The use of IgG Fc to target the NPs to FcRn resulted in absorption efficiency 11.5-fold higher than for nontargeted NPs, but the efficiency could potentially be higher, as some ^{14}C could have been absorbed in other tissues not measured in these studies. Furthermore, insNPs targeting FcRn, a model NP-based therapeutic for the treatment of diabetes, were able to generate a hypoglycemic response after oral administration at a clinically relevant insulin dose that is significantly lower than the doses required by other drug delivery systems designed for oral insulin delivery (29). Moreover, rodents significantly downregulate the FcRn expression in the intestine after weaning (35), but humans continue to express FcRn into adulthood. Therefore, while NP-Fc can increase transepithelial transport in mice, the transport in humans could potentially be even more efficient.

There are some potential limitations to this technology that need to be investigated. For example, FcRn is expressed in many tissues in addition to the intestine. Using IgG Fc to target the FcRn could potentially result in uptake in tissues other than the targeted tissue. However, FcRn expression in tissues such as the vascular endothelium, blood-brain barrier, and lungs could also allow the technology to be expanded for drug delivery across other cellular barriers. Immunological responses to Fc on the NP surface need to be investigated as well. The presence of IgG Fc may result in faster blood clearance of the NPs due to interactions with Fc receptors. NP-Fc may also generate immunological responses and thus could potentially be used for oral vaccine applications (36).

This technology may have a major impact on the treatment of several diseases by enabling NP-based therapies to be orally administered. In addition, the encapsulation of drugs or biologics that are currently limited by low bioavailability into NPs that target FcRn may enable markedly more efficient oral delivery of the therapies. The path forward for translation of this technology to the clinic is to test the NP-Fc in larger animal models such as pigs and non-human primates. Some key parameters that need to be understood for success in the clinic are the ideal release profile for an oral insulin formulation and how absorption varies based on diet and patient-to-patient variability.

Materials and Methods

Synthesis of Polymers

D,L-Lactide (Sigma-Aldrich) and MAL-PEG-OH (JenKem Technology) were used to synthesize PLA-PEG-MAL by ring opening polymerization. D,L-Lactide (3 g, 20.8 mmol) and MAL-PEG-OH (544 mg, 0.16 mmol) were dissolved in 15 mL anhydrous toluene in a round bottom flask. Tin(II) ethylhexanoate (38 mg, 0.09 mmol) was then added. The flask with condenser was placed in an oil bath, purged with nitrogen for 10 minutes, heated to 120°C, and reacted overnight while 4°C water circulated through the condenser. Toluene was then evaporated and the polymer precipitated in a 50:50 (v/v) mixture of ice-cold methanol and diethyl ether and vacuum-dried. The PLA-PEG-MAL was characterized by ^{1}H NMR (400 MHz), δ = 5.28–5.11 (br, -OC-C*H*(CH_3)O- in PLA), 3.62 (s, -CH_2CH_2O- in PEG), 1.57–1.45 (br, -OC-CHCH_3O- in PLA). Using GPC, the polymer M_n = 12.5 kDa with M_w/M_n = 1.47 relative to polystyrene standards. Poly(lactic acid) (PLA) (inherent viscosity 0.50 dL/g) with terminal carboxylate groups (Lactel) was conjugated to ^{14}C doxorubicin (Perkin Elmer) (PLA-^{14}C) and Alexa Fluor 647 (AF647) hydrazide tris(triethylammonium) salt (Invitrogen) (PLA-AF647) were prepared the same way. PLA (30 mg, 0.83 μmol) in 1 mL dimethylformamide (DMF) was reacted with N-hydroxysuccinimide (NHS) (0.5 mg, 4.2 μmol) in the presence of 1-ethyl-3-[3-dimethylaminopropyl] (0.8 mg, 4.2 μmol) overnight. PLA-NHS was precipitated in a 50:50 (v/v) mixture of ice-cold methanol and diethyl ether and vacuum-dried. For PLA-^{14}C, PLA-NHS (18 mg, 0.5 μmol) was mixed overnight with ^{14}C Doxorubicin (0.27 mg, 0.5 μmol) in 1 mL DMF. For PLA-AF647, PLA-NHS (50 mg, 1.4 μmol) was mixed overnight with Alexa Fluor 647 (1.5 mg, 1.4 μmol) in 1 mL DMF. Both polymers were precipitated in a mixture of 50:50 (v/v) ice-cold methanol and diethyl ether and vacuum-dried.

Synthesis and characterization of NP-Fc

To prepare the NP-Fc, 3 mg PLA-PEG-MAL was dissolved in 300 μL acetonitrile and added dropwise to 1.5 mL water. The solution was mixed for 2 h, and the NPs were purified by filtration using Millipore Amicon Ultra 100,000 NMWL. The NPs were washed 2x with water and 2x with phosphate-buffered saline (PBS) containing 5 mM EDTA. Concurrently, 86 μg of purified human polyclonal IgG Fc prepared by papain digestion (Bethyl Laboratories) or 95 μg of chicken IgY Fc (Jackson ImmunoResearch Laboratories) in PBS containing 5 mM EDTA was reacted with 0.48 μL of 5 mg/mL 2-iminothiolane (Traut's Reagent) for 1 h. The modified Fc was added to the NPs and mixed for 1 h to allow conjugation at 4°C. The NP-Fc were washed with PBS using Millipore Amicon Ultra

100,000 NMWL. The conjugation of IgG Fc to the NP surface was measured using a protein bicinchoninic acid (BCA) assay from Lamda Biotech. Particle diameter and surface charge (zeta potential) were measured using dynamic light scattering with a Brookhaven Instruments ZetaPALS.

In vitro Transcytosis Studies

Transepithelial transport studies utilized Transwell plates (Costar) with a Caco-2 (American Type Culture Collection - ATCC) cell density of 5.5×10^4 in media [ATCC formulated Eagle's Minimum Essential Medium with aqueous penicillin G (100 units/mL), streptomycin (100 U/mL), and fetal bovine serum (FBS, 20%)]. On the day of the transport experiment, the media was changed to HBSS pH 6.5 in the apical chamber and HBSS pH 7.4 in the basolateral chamber and allowed to equilibrate for 1 h at 37°C and 5% CO_2. Prior to the experiment and at the end of the experiment, the monolayer integrity was checked by measuring the transepithelial resistance (TEER) using a Millicell-ERS (Millipore). TEER values were 900–1000 Ω/cm^2 for wells used in transport experiments and the TEER remained constant throughout the experiments. ^{3}H-labeled NPs were prepared by blending 50 μg ^{3}H-poly(lactic-*co*-glycolic acid) (PLGA) (Perkin Elmer) with 1 mg PLA-PEG-MAL in 100 μL acetonitrile prior to nanoprecipitation in 500 μL water and then washed in HBSS pH 6.5 prior to the transport experiment. The apical solution was then replaced with a solution of 100 μg ^{3}H-labeled NPs or NP-Fc in 250 μL HBSS pH 6.5. The NP formulations were incubated for 24 h before measuring the ^{3}H content in the basolateral chamber. The basolateral solution was collected and added to a Hionic-Fluor scintillation cocktail (Perkin Elmer) before analysis using a Packard Tri-Carb Scintillation Analyser. At the end of the experiment, the TEER was measured again to verify monolayer integrity. For the IgG Fc blocking experiment, a 50x molar excess of IgG Fc relative to Fc on the NP-Fc surface was added concurrently with NP-Fc to the apical chamber, and the ^{3}H content in the basolateral chamber was measured after 24 h.

Western Blot

Sections of small intestine and colon were removed from wild-type mice after euthanasia. Intestinal epithelial cells were isolated (37, 38) and the protein was extracted. Protein concentrations in the extracts were determined using the BCA assay. Extracts were resolved on a 12% SDS-PAGE gel under reducing conditions. Proteins were transferred onto a nitrocellulose membrane. The membrane was blocked with 5% nonfat milk, probed with rabbit anti-mouse FcRn (Santa Cruz Biotech) for 1 h, and then incubated with goat anti-rabbit IgG-HRP (Santa Cruz Biotech). All blocking, incubations, and washes used PBS-T (PBS with 0.05% Tween 20). Detection was by chemiluminescence. Band intensity was quantified using ImageJ.

Immunohistochemistry

Small intestine tissues were harvested and fixed in 10% formalin overnight. After ethanol dehydration, tissues were paraffin embedded and cut into 8 μm-thick sections, mounted on slides, and dried overnight. The tissues were then rehydrated using xylene and ethanol. Endogenous peroxidase activity, endogenous biotin, and nonspecific proteins were blocked

with 3% H_2O_2, avidin blocking agent, and 10% goat serum, respectively. The samples were incubated with polyclonal rabbit IgG or anti-mouse FcRn IgG (Santa Cruz Biotech) primary antibody overnight, then incubated with biotinylated anti-rabbit secondary antibodies (Santa Cruz Biotech), with streptavidin-HRP, developed with DAP, and mounted with hematoxylin counterstain.

In vivo Fluorescence Imaging

All animal studies were conducted under the supervision of MIT's Division of Comparative Medicine in compliance with the NIH's *Principles of Laboratory Animal Care*. Wild-type Balb/c mice (Charles River Laboratories) (n=3) were fasted overnight prior to gavage. Fluorescently-labeled NPs were prepared by blending 100 μg PLA-AF647 with 1 mg PLA-PEG-MAL in 100 μL acetonitrile prior to nanoprecipitation in 500 μL water. Fluorescently-labeled NP and NP-Fc were washed 3x in water until the flow-through was clear and suspended in 200 μL water (7 mL water/kg). The suspension was then administered to the mice by oral gavage. After 1.5 h, the mice were euthanized. Duodenum tissue sections were, frozen into Tissue-Tek OCT using liquid nitrogen. Cross sections of the tissue were obtained using a Leica CM1900 Cryostat with a thickness of 12 μm. The tissue was air-dried overnight and then stained with Prolong Gold (Life Technologies) antifade reagent with 4′, 6-diamidino-2-phenylindole (DAPI). Fluorescent images were obtained using a Zeiss LSM 710 NLO scanning confocal microscope under oil immersion at 40x magnification.

In vivo Biodistribution

To prepare ^{14}C-labeled NPs, 450 μg PLA-^{14}C was blended with 3 mg PLA-PEG-MAL in 300 μL acetonitrile prior to nanoprecipitation in 1.5 mL water. NPs were washed 2x with water and 2x with PBS. ^{14}C release was measured by preparing a batch of ^{14}C NPs in PBS with pH 7.4 and dividing the batch equally into 500 μg samples for incubation at 37°C. At each timepoint, samples were collected, washed 3x with PBS using Millipore Amicon Ultra 100,000 NMWL, and then added to 15 mL of Hionic Fluor scintillation cocktail. The activity was counted using a Packard Tri-Carb Scintillation Analyser. For the *in vivo* biodistribution experiments, 6–12 week old wild-type mice were fasted 8 h prior to oral gavage of 1.5 mg (0.1 μCi/mouse) of ^{14}C-labeled NP and NP-Fc in 7 mL PBS/kg. Groups of mice (n=5 mice) were euthanized at each time point, and the spleen, kidneys, liver, lungs, and heart were harvested. Each organ was placed directly in a scintillation vial except for the liver, which was homogenized and ~100 mg was analyzed. Each organ was solubilized in 2 mL of Solvable (Perkin Elmer) for 12 h at 60°C and then decolored with 200 μL of 0.5 M EDTA (Invitrogen) and 200 μL 30% hydrogen peroxide (Fisher Scientific) for 1 h at 60°C. The activity was counted in 15 mL Hionic-Fluor scintillation cocktail using a Packard Tri-Carb Scintillation Analyser. To determine 100% dose, vials of 500 μg NPs and NP-Fc were counted in 15 mL Hionic-Fluor scintillation cocktail. For the oral absorption efficiency, total ^{14}C counted in all tissues was added at each time point. The AUC of total absorbed ^{14}C versus time was calculated using the trapezoid method and divided by the initial dose to determine the oral absorption efficiency. The results were reported as mean ± SEM, and comparison of non-targeted NPs and NP-Fc utilized the two-tailed Student's t-test.

Insulin Encapsulation and Release

Insulin NPs were prepared by blending 900 μg human recombinant insulin (Sigma-Aldrich), 450 μg PLGA (50:50 G:L, inherent viscosity 0.20 dL/g) with terminal carboxylate groups (Lactel), and 3 mg PLA-PEG-MAL together in 525 μL dimethyl sulfoxide (DMSO) prior to nanoprecipitation in 2.1 mL water. Free insulin was removed using Millipore Amicon Ultra 100,000 NMWL by washing 2x with water and 2x with PBS. Insulin encapsulation was measured by heating the NPs to 60°C for 30 min, and insulin was quantified using a BCA assay or insulin ELISA kit (Millipore). Insulin release from the NP was measured by dividing a batch of insNP equally into 24 kDa dialysis units (Pierce) and incubating at 37°C in PBS with pH 7.4. At each timepoint, three samples of insNP were collected, washed with PBS using Millipore Amicon Ultra 100,000 NMWL, heated to 60°C for 30 min, and measured for insulin using a BCA assay.

Insulin Activity

Insulin activity was measured by preparing insNP and allowing insulin release for 2 h at 37°C in PBS at pH 7.4. Wild-type mice were fasted for 8 h, and the mice (n=3/group) used were chosen so that the mean initial blood glucose levels were the same for each group. 3.3 U/kg of released insulin was administered to the fasted mice by tail-vein injection. An equivalent dose of free insulin by mass was administered by tail-vein injection to another group of fasted mice. The blood glucose level was measured using the Contour blood glucose monitor (Bayer).

In vivo Efficacy

6–12-week old wild-type or FcRn knockout (39) mice (Jackson Laboratories) were fasted for 8 hours. Mice (n=5–6) were chosen per group such that the mean initial blood glucose levels were the same per group. 150 or 250 μg of insNP or insNP-Fc (insulin dose −0.66 or 1.1 U/kg) in 7 mL PBS/kg were administered to the mice by oral gavage. For controls, 1.1 U/kg of free insulin and 250 μg of NP-Fc without insulin in 7 mL PBS/kg were administered by oral gavage. For the excess IgG Fc control, 250 μg of insNP-Fc was formulated with 50x molar excess of IgG Fc in 7 mL PBS/kg prior to administration to the mice by oral gavage The blood glucose level was measured as described above.

Statistical Analysis

All data are presented as means with either SD or SEM as indicated. Statistical significance was determined by a two-tailed Student's t test ($\alpha = 0.05$) assuming equal variance.

Acknowledgments

We thank the W.M Keck Microscope Facility at the Whitehead Institute, in particular Wendy Salmon for her assistance with the fluorescence microscopy imaging. We thank Benjamin Tang for his help with the confocal microscopy image analysis.

Funding: Supported in part by a Koch-Prostate Cancer Foundation Award in Nanotherapeutics (R.L. and O.C.F.), the NCI Center of Cancer Nanotechnology Excellence at MIT-Harvard (U54-CA151884), a NHLBI PEN Award (Contract # HHSN268201000045C), NIH grant EB000244, and an NIH R01 grant (EB015419-01). R.S.B. is supported by NIH DK53056 and a Harvard Digestive Disease Center (HDDC) Grant (DK0034854). E.M.P is supported by a NDSEG graduate research fellowship and a Center of Cancer Nanotechnology Excellence graduate research fellowship (5 U54 CA151884-02).

References

1. Davis ME, Zuckerman JE, Choi CHJ, Seligson D, Tolcher A, Alabi CA, Yen Y, Heidel JD, Ribas A. Evidence of RNAi in humans from systemically administered siRNA via targeted nanoparticles. Nature. 2010; 464:1067–1070. [PubMed: 20305636]
2. Wang AZ, Langer R, Farokhzad OC. Nanoparticle Delivery of Cancer Drugs. Annu Rev Med. 2012; 63:185–198. [PubMed: 21888516]
3. Hrkach J, Von Hoff D, Ali MM, Andrianova E, Auer J, Campbell T, De Witt D, Figa M, Figueiredo M, Horhota A, Low S, McDonnell K, Peeke E, Retnarajan B, Sabnis A, Schnipper E, Song JJ, Song YH, Summa J, Tompsett D, Troiano G, Van Geen Hoven T, Wright J, LoRusso P, Kantoff PW, Bander NH, Sweeney C, Farokhzad OC, Langer R, Zale S. Preclinical Development and Clinical Translation of a PSMA-Targeted Docetaxel Nanoparticle with a Differentiated Pharmacological Profile. Sci Transl Med. 2012; 4:128ra39–128ra39.
4. Farokhzad OC, Cheng J, Teply BA, Sherifi I, Jon S, Kantoff PW, Richie JP, Langer R. Targeted nanoparticle-aptamer bioconjugates for cancer chemotherapy in vivo. Proc Natl Acad Sci U S A. 2006; 103:6315–6320. [PubMed: 16606824]
5. Borner MM, Schoffski P, de Wit R, Caponigro F, Comella G, Sulkes A, Greim G, Peters GJ, van der Born K, Wanders J, de Boer RF, Martin C, Fumoleau P. Patient preference and pharmacokinetics of oral modulated UFT versus intravenous fluorouracil and leucovorin: a randomised crossover trial in advanced colorectal cancer. Eur J Cancer. 2002; 38:349–358. [PubMed: 11818199]
6. Goldberg M, Gomez-Orellana I. Challenges for the oral delivery of macromolecules. Nat Rev Drug Discov. 2003; 2:289–295. [PubMed: 12669028]
7. Yoshida M, Claypool SM, Wagner JS, Mizoguchi E, Mizoguchi A, Roopenian DC, Lencer WI, Blumberg RS. Human neonatal Fc receptor mediates transport of IgG into luminal secretions for delivery of antigens to mucosal dendritic cells. Immunity. 2004; 20:769–783. [PubMed: 15189741]
8. Dickinson BL, Badizadegan K, Wu Z, Ahouse JC, Zhu X, Simister NE, Blumberg RS, Lencer WI. Bidirectional FcRn-dependent IgG transport in a polarized human intestinal epithelial cell line. J Clin Invest. 1999; 104:903–911. [PubMed: 10510331]
9. Brambell FW. The transmission of immune globulins from the mother to the foetal and newborn young. Proc Nutr Soc. 1969; 28:35–41. [PubMed: 4182340]
10. Israel EJ, Taylor S, Wu Z, Mizoguchi E, Blumberg RS, Bhan A, Simister NE. Expression of the neonatal Fc receptor, FcRn, on human intestinal epithelial cells. Immunology. 1997; 92:69–74. [PubMed: 9370926]
11. Kuo TT, Aveson VG. Neonatal Fc receptor and IgG-based therapeutics. MAbs. 2011; 3:422–430. [PubMed: 22048693]
12. Baker K, Qiao SW, Kuo TT, Aveson VG, Platzer B, Andersen JT, Sandlie I, Chen Z, de Haar C, Lencer WI, Fiebiger E, Blumberg RS. Neonatal Fc receptor for IgG (FcRn) regulates cross-presentation of IgG immune complexes by CD8-CD11b+ dendritic cells. Proc Natl Acad Sci USA. 2011; 108:9927–9932. [PubMed: 21628593]
13. Raghavan M, Gastinel LN, Bjorkman PJ. The class I major histocompatibility complex related Fc receptor shows pH-dependent stability differences correlating with immunoglobulin binding and release. Biochemistry. 1993; 32:8654–8660. [PubMed: 8357807]
14. He W, Ladinsky MS, Huey-Tubman KE, Jensen GJ, McIntosh JR, Björkman PJ. FcRn-mediated antibody transport across epithelial cells revealed by electron tomography. Nature. 2008; 455:542–546. [PubMed: 18818657]
15. Lalezari, David. Gastrointestinal pH profile in subjects with irritable bowel syndrome. Ann Gastroenterol. 2012; 25:1–5. [PubMed: 24713794]
16. Roopenian DC, Akilesh S. FcRn: the neonatal Fc receptor comes of age. Nat Rev Immunol. 2007; 7:715–725. [PubMed: 17703228]
17. Dickinson BL, Claypool SM, D'Angelo JA, Aiken ML, Venu N, Yen EH, Wagner JS, Borawski JA, Pierce AT, Hershberg R. Ca2+-dependent calmodulin binding to FcRn affects immunoglobulin G transport in the transcytotic pathway. Mol Biol Cell. 2008; 19:414–423. [PubMed: 18003977]

18. Ober RJ, Martinez C, Lai X, Zhou J, Ward ES. Exocytosis of IgG as mediated by the receptor, FcRn: an analysis at the single-molecule level. Proc Natl Acad Sci U S A. 2004; 101:11076. [PubMed: 15258288]

19. Bitonti AJ, Dumont JA, Low SC, Peters RT, Kropp KE, Palombella VJ, Stattel JM, Lu Y, Tan CA, Song JJ. others, Pulmonary delivery of an erythropoietin Fc fusion protein in non-human primates through an immunoglobulin transport pathway. Proc Natl Acad Sci U S A. 2004; 101:9763. [PubMed: 15210944]

20. Dumont JA, Bitonti AJ, Clark D, Evans S, Pickford M, Newman SP. Delivery of an erythropoietin-Fc fusion protein by inhalation in humans through an immunoglobulin transport pathway. J Aerosol Med. 2005; 18:294–303. [PubMed: 16181004]

21. Low SC. Oral and pulmonary delivery of FSH-Fc fusion proteins via neonatal Fc receptor-mediated transcytosis. Hum Reprod. 2005; 20:1805–1813. [PubMed: 15817590]

22. Vllasaliu D, Alexander C, Garnett M, Eaton M, Stolnik S. Fc-mediated transport of nanoparticles across airway epithelial cell layers. J Control Release. 2012; 158:479–486. [PubMed: 22200577]

23. Awaad A, Nakamura M, Ishimura K. Imaging of size-dependent uptake and identification of novel pathways in mouse Peyer's patches using fluorescent organosilica particles. Nanomedicine: NBM. 2012; 8:627–636.

24. Desai MP, Labhasetwar V, Amidon GL, Levy RJ. Gastrointestinal uptake of biodegradable microparticles: effect of particle size. Pharm Res. 1996; 13:1838–1845. [PubMed: 8987081]

25. Bilati U, Allémann E, Doelker E. Nanoprecipitation versus emulsion-based techniques for the encapsulation of proteins into biodegradable nanoparticles and process-related stability issues. AAPS Pharm Sci Tech. 2005; 6:E594–E604.

26. Armstrong JK, Wenby RB, Meiselman HJ, Fisher TC. The Hydrodynamic Radii of Macromolecules and Their Effect on Red Blood Cell Aggregation. Biophys J. 2004; 87:4259–4270. [PubMed: 15361408]

27. Liu X, Ye L, Christianson GJ, Yang JQ, Roopenian DC, Zhu X. NF-kappaB signaling regulates functional expression of the MHC class I-related neonatal Fc receptor for IgG via intronic binding sequences. J Immunol. 2007; 179:2999–3011. [PubMed: 17709515]

28. Cochran E, Musso C, Gorden P. The use of U-500 in patients with extreme insulin resistance. Diabetes Care. 2005; 28:1240–1244. [PubMed: 15855601]

29. Chen MC, Sonaje K, Chen KJ, Sung HW. A review of the prospects for polymeric nanoparticle platforms in oral insulin delivery. Biomaterials. 2011; 32:9826–9838. [PubMed: 21925726]

30. Israel EJ, Wilsker DF, Hayes KC, Schoenfeld D, Simister NE. Increased clearance of IgG in mice that lack β2-microglobulin: possible protective role of FcRn. Immunology. 1996; 89:573–578. [PubMed: 9014824]

31. Salama N, Eddington N, Fasano A. Tight junction modulation and its relationship to drug delivery. Adv Drug Deliv Rev. 2006; 58:15–28. [PubMed: 16517003]

32. Smart J. The basics and underlying mechanisms of mucoadhesion. Adv Drug Deliv Rev. 2005; 57:1556–1568. [PubMed: 16198441]

33. Shakweh M, Ponchel G, Fattal E. Particle uptake by Peyer's patches: a pathway for drug and vaccine delivery. Expert Opin Drug Deliv. 2004; 1:141–163. [PubMed: 16296726]

34. Jain S, Rathi VV, Jain AK, Das M, Godugu C. Folate-decorated PLGA nanoparticles as a rationally designed vehicle for the oral delivery of insulin. Nanomed. 2012; 7:1311–1337.

35. Martín MG, Wu SV, Walsh JH. Ontogenetic development and distribution of antibody transport and Fc receptor mRNA expression in rat intestine. Dig Dis Sci. 1997; 42:1062–1069. [PubMed: 9149063]

36. Ye L, Zeng R, Bai Y, Roopenian DC, Zhu X. Efficient mucosal vaccination mediated by the neonatal Fc receptor. Nat Biotechnol. 2011; 29:158–163. [PubMed: 21240266]

37. Booth, C.; O'Shea, JA. Culture of Epithelial Cells. Wiley-Liss, Inc; 2002. p. 303-335.

38. Pan D, Das A, Liu D, Veazey RS, Pahar B. Isolation and characterization of intestinal epithelial cells from normal and SIV-infected rhesus macaques. PloS One. 2012; 7:e30247. [PubMed: 22291924]

39. Roopenian DC, Christianson GJ, Sproule TJ, Brown AC, Akilesh S, Jung N, Petkova S, Avanessian L, Choi EY, Shaffer DJ, Eden PA, Anderson CL. The MHC class I-like IgG receptor

controls perinatal IgG transport, IgG homeostasis, and fate of IgG-Fc-coupled drugs. J Immunol. 2003; 170:3528–3533. [PubMed: 12646614]

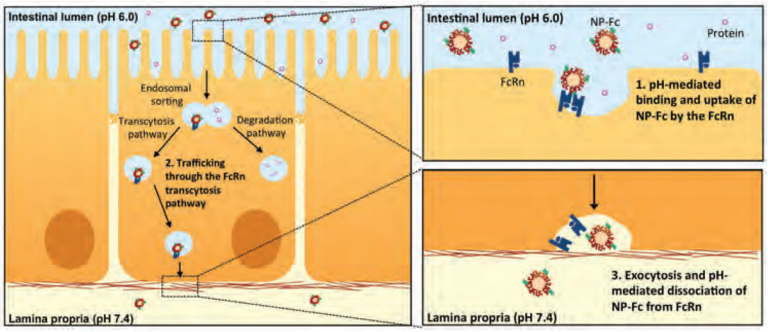

Fig. 1. Schematic of Fc-targeted nanoparticle transport across the intestinal epithelium by the FcRn through a transcytosis pathway

(1) IgG Fc on the NP surface binds to the FcRn on the apical side of absorptive epithelial cells under acidic conditions in the intestine. (2) NP-Fc are then trafficked across the epithelial cell through the FcRn transcytosis pathway in acidic endosomes. (3) Upon exocytosis on the basolateral side of the cell, the physiological pH causes IgG Fc to dissociate from the FcRn, and NP-Fc are free to diffuse through the intestinal lamina propria to the capillaries or lacteal and enter systemic circulation.

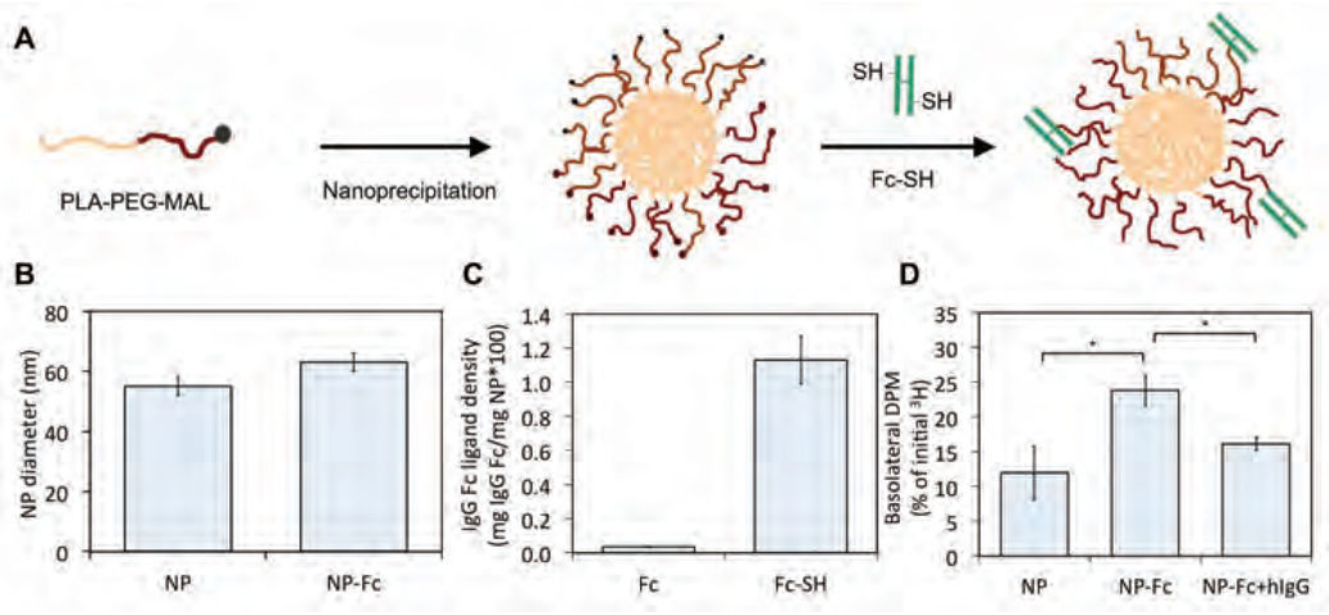

Fig. 2. Nanoparticle assembly, characterization, and *in vitro* transepithelial transport

(**A**) Schematic of NP-Fc assembly. NPs consist of a biodegradable PLA core for drug encapsulation and a PEG surface coating for particle stability and to reduce phagocytic uptake. NPs were formed using the nanoprecipitation self-assembly method (25) and surface-modified with IgG Fc for FcRn targeting. (**B**) Dynamic light scattering measurements for non-targeted NPs and NP-Fc. Data are means ± SD (n=3). (**C**) IgG Fc ligand density on the NP surface with (Fc-SH) and without (Fc) thiol modification of the IgG Fc. Data are means ± SD (n=3). (**D**) *In vitro* transepithelial transport of non-targeted NPs, NP-Fc, and NP-Fc with an excess of human IgG Fc as a blocking agent for FcRn. Data are expressed as mean basolateral ^{3}H disintegrations per minute (DPM) as a percentage of the initial amount of ^{3}H (± SEM; n = 4 wells per group). *P < 0.05, two-tailed Student's t-test.

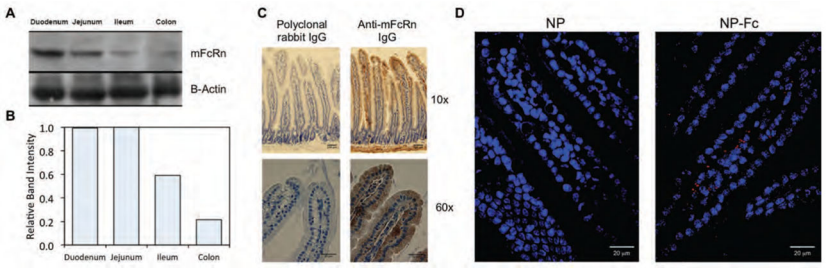

Fig. 3. FcRn expression and nanoparticle intestinal uptake in mice

(**A**) Western blot of mouse FcRn (mFcRn) in mouse intestinal tissue. (**B**) Quantification of Western blot band intensity. The relative band intensity was calculated as the ratio of mFcRn to B-Actin band intensity from the Western Blot. (**C**) Immunohistochemistry on sections of mouse duodenum. mFcRn appears brown. The negative control was tissue stained with polyclonal IgG. (**D**) Fluorescently labeled NPs (red) were administered to fasted wild-type mice by oral gavage and the intestines were collected for sectioning and imaging 1.5 h after administration. The panels are confocal fluorescence images of 12-μm sections of mouse duodenum. Cell nuclei were stained with DAPI (blue). Images are representative for n=3 mice.

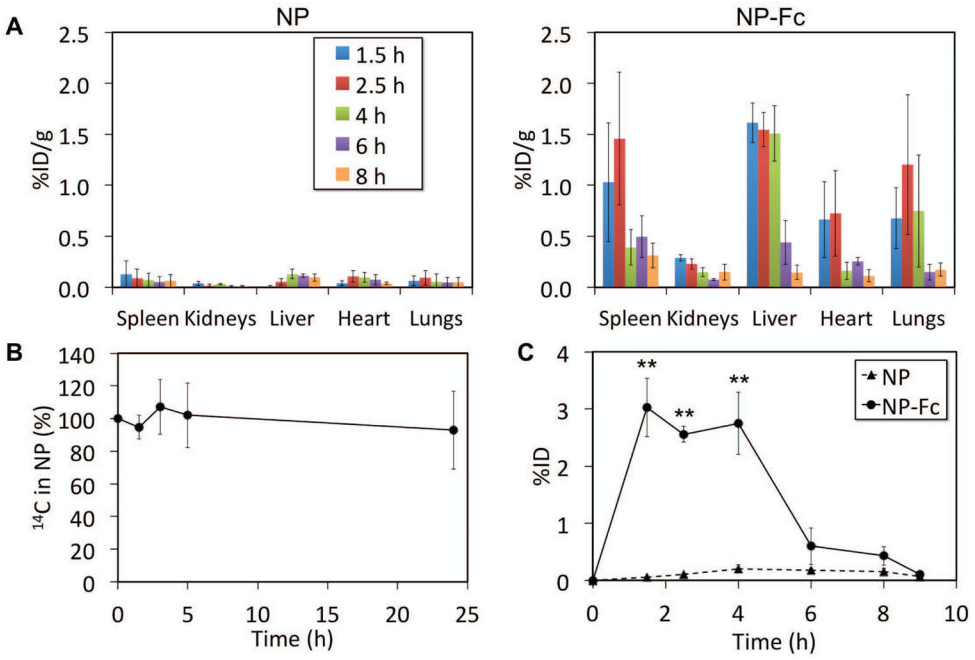

Fig. 4. Nanoparticle absorption and biodistribution in mice

(**A**) Biodistribution of ^{14}C-labeled non-targeted NPs and NP-Fc after oral administration to fasted wild-type mice. Data are mean % initial dose (ID) per gram of tissue ± SEM (n=5 mice per time point). (**B**) Release of ^{14}C from ^{14}C-labeled NPs in PBS at 37°C. Data are means ± SD for n=4 release experiments. (**C**) Total absorbed ^{14}C over time for non-targeted NPs and NP-Fc after administration by oral gavage. Data are mean %ID measured in all of the organs added together ± SEM (n=5 mice per time point). **P < 0.01 for comparison of non-targeted NPs and NP-Fc at respective time point, two-tailed Student's t-test.

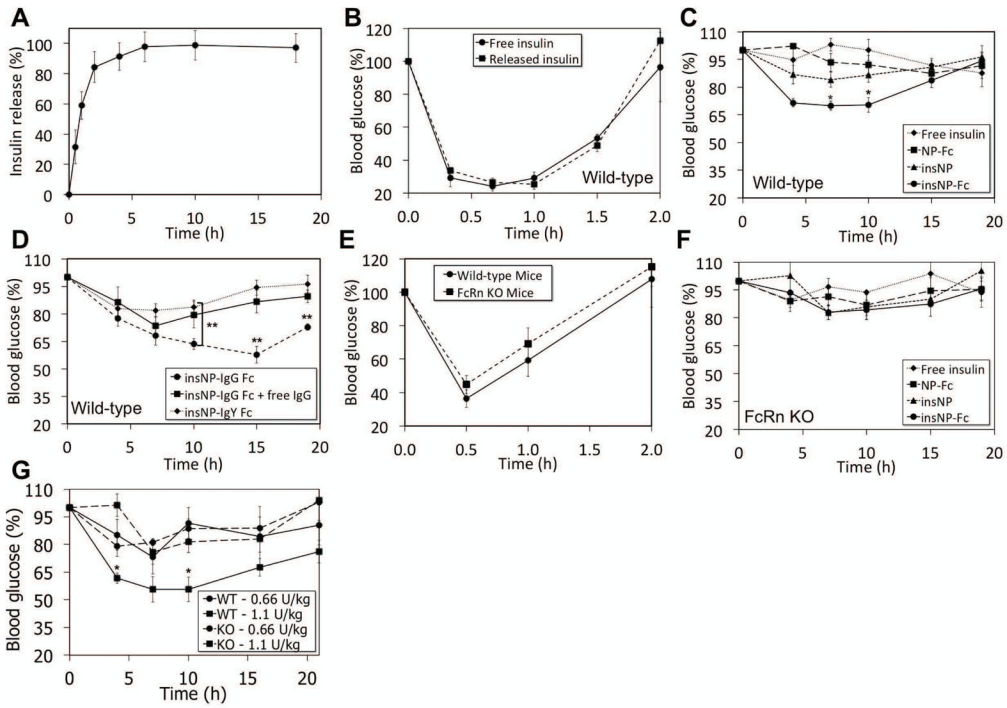

Fig. 5. Encapsulation of insulin and oral delivery of Fc-targeted insulin nanoparticles to mice

(**A**) Release of insulin from insNP into PBS. Data are means ± SD (n=3 per time point). (**B**) Blood glucose response of fasted wild-type mice to insulin encapsulated and released from NPs in (A) before administration. Fasted wild-type mice received free insulin (3.3 U/kg) administered by tail-vein injection. Data are means ± SEM (n=3 mice per group). (**C**) Blood glucose response of fasted wild-type mice to free insulin solution, NP-Fc containing no insulin, non-targeted insNP, and insNP-Fc, each administered by oral gavage. Data are means ± SEM (n=6 mice per group). *P < 0.05 for comparison of non-targeted insNP and insNP-Fc at corresponding time points, two-tailed Student's t-test. (**D**) Blood glucose response of fasted wild-type mice to insNP-Fc, insNP-Fc administered concurrently with excess of IgG Fc, and insNP with chicken IgY Fc fragments, each administered by oral gavage. Data are means ± SEM (n=5 mice per group). **P<0.01 for comparison between insNP-Fc with insNP-Fc + free IgG Fc at the 15 and 19 h timepoints and between insNP-IgG Fc and insNP-IgY Fc at the 10, 15, and 19 h timepoints using a two-tailed Student's t-test. (E) Blood glucose response to equivalent insulin doses (3.3 U/kg) administered by tail-vein injection into fasted wild-type and FcRn KO mice. Data are means ± SEM (n=3 mice per group). (**F**) Fasted FcRn KO mice blood glucose response to free insulin solution, NP-Fc containing no insulin, non-targeted insNP, or insNP-Fc, each administered by oral gavage. Data are means ± SEM (n=5 mice per group). (**G**) Fasted wild-type and FcRn KO mice were dosed by oral gavage with non-targeted insNP and insNP-Fc at two different doses. *P<0.05 for comparison between insNP-Fc at 1.1 U/kg and each of the other groups at corresponding timepoints, two-tailed Student's t-test.